Mechanisms of endoplasmic reticulum export of the glycine transporter GLYT1

Enrique Fernández-Sánchez, F Javier Díez-Guerra, Beatriz Cubelos, Cecilio Giménez, Francisco Zafra

Mechanisms of endoplasmic reticulum export of the glycine transporter GLYT1

Enrique FERNÁNDEZ-SÁNCHEZ, F. Javier DÍEZ-GUERRA, Beatriz CUBELOS, Cecilio GIMÉNEZ and Francisco ZAFRA[1]

Centro de Biología Molecular "Severo Ochoa", Facultad de Ciencias, Universidad Autónoma de Madrid and Consejo Superior de Investigaciones Científicas, 28049-Madrid, Spain.

Short title: ER export of GLYT1

[1] To whom correspondence should be addressed: Dr. F. Zafra, Centro de Biología Molecular "Severo Ochoa", Facultad de Ciencias, Universidad Autónoma de Madrid, 28049 Madrid, Spain.

Phone: 34-914978720; Fax: 34-914974799; E-mail: fzafra@cbm.uam.es

Key words: neurotransmitter transporters; endoplasmic reticulum; protein traffic; COPII; neurotransmission.

The glycine transporter GLYT1 regulates both glycinergic and glutamatergic neurotransmission by controlling the reuptake of glycine at synapses. Trafficking to the cell surface of GLYT1 is critical for its function. In this article, by using mutational analysis of the GLYT1 C-terminal domain we identified the evolutionary conserved motif $R^{575}L^{576}(X_8)D^{585}$ as being necessary for endoplasmic reticulum (ER) export. This is probably due to its capacity to bind Sec24D, a component of the COPII complex. This ER export motif was active when introduced into the related GLYT2 transporter but not in the unrelated VSVG protein. GLYT1 protein in which this motif was mutated was not transported to the plasma membrane, although this effect was rescued by co-expressing these mutants with wild-type GLYT1. This behavior suggests that GLYT1 might form oligomers along the trafficking pathway. Cross-linking assays performed in rat brain synaptosomes, and Fluorescence Resonance Energy Transfer (FRET) microscopy in living cells confirmed the existence of GLYT1 oligomers. In summary, we have identified a motif involved in the ER exit of GLYT1 and in analyzing the influence of this motif, we have found evidence that oligomerization is important for the trafficking of GLYT1 to the cell surface. Because this motif is conserved in the NSS family, it is possible that this finding could be extrapolated to other related transporters.

INTRODUCTION

Beside its well-characterized role as an inhibitory neurotransmitter, glycine is a co-agonist of NMDA receptors (NMDAR) which is necessary for ion channel opening and probably, for the internalization of the receptor from the cell surface [1, 2]. While it was initially believed that the concentration of glycine in the synaptic cleft would be high enough to saturate the glycine sites on NMDAR, recent pharmacological and electrophysiological evidence indicates that due to the activity of the GLYT1 glycine transporter, this might be not the case. GLYT1 seems to fulfill a dual role in neurotransmission. First, it is highly expressed in glycinergic areas of the nervous system where it is predominantly found in glial cells, and is associated to glycinergic inhibitory neurotransmission [3, 4]. Secondly, GLYT1 is present in neuronal elements closely associated with the glutamatergic pathways throughout the brain [5]. Functional and anatomical evidence strongly support a role of GLYT1 in regulating NMDAR-mediated neurotransmission. [5-12].

The mechanisms responsible for the insertion of GLYT1 into glutamatergic or glycinergic synapses are unknown. However, recent studies indicate that the movement of transporters within the cell is highly organized and that a number of ancillary proteins control their intracellular trafficking, interacting with targeting motifs in the sequence of the transporter. Indeed, GLYT1, like other neurotransmitter transporters, is asymmetrically distributed in polarized cells [13, 14]. The asymmetrical distribution of NSS transporters requires a number of steps that commence with their efficient exit from the ER. This is followed by sorting processes in the Golgi complex, insertion into the plasma membrane, and retention of the transporter at functional synaptic sites. Moreover, the amount of transporter in the plasma membrane is also regulated by endocytosis and recycling mechanisms. Among these steps, export of polytopic proteins from the ER, such as NSS transporters, is poorly characterized. Such ER export does require specific signals in the amino acidic sequence and posttranslational modifications that probably include glycosylation and oligomerization. These mechanisms might help to pass the stringent quality control in the ER which rejects misfolded proteins [reviewed in 15]. We have shown that half of the C-terminal domain of GLYT1 that lies closest to the plasma membrane is necessary for ER export of this protein [16]. In addition, mutations in the PDZ interacting motif Ser-Arg-Ile present in the C-terminus

of GLYT1 delays its delivery to the plasma membrane [6]. Similarly, ER export of the dopamine transporter and the GABA transporter GAT1 is also dependent on the cooperation of two discontinuous segments located in the C-terminal domain: one corresponding to the last three residues (also a PDZ-binding motif) and another to a sequence segment adjacent to the twelfth transmembrane helix [17, 18, 19]. Extensive mutagenesis of this second region in DAT revealed that mutating Gly-585, Lys-590 or Asp-600 led to the protein retention in the ER [20]. A further step in the understanding of ER export of this family of transporter has been recently reported by the group of H. Sitte who found that mutations in the sequence R566L567, located in the C-terminus of the GABA transporter GAT1, disturb the interaction of this transporter with Sec24D, a component of the COPII complex [21].

Oligomer formation of newly synthesized transporters has been suggested as an essential step in ER exit. Biochemical experiments including radiation inactivation, chromatography filtration of detergent solubilized proteins, coimmunoprecipitation and cross-linking studies have provided evidence that SERT, DAT and the norepinephrine transporter (NET) form oligomeric complexes [22-28]. Moreover, assays using dominant negative forms of these three transporters have produced data compatible with the existence of transporter oligomers [18, 29, 30]. Additional evidence for the formation of oligomers for the GABA transporter GAT1, SERT and DAT has also been obtained in living cells by FRET microscopy [25, 31]. These transporters not only exist as oligomers in the plasma membrane, but also through the biosynthetic and protein trafficking pathway. Hence, only properly assembled transporters might be able to recruit the coatomer coat proteins (COPII) needed for ER export. However, biochemical analysis of GLYT1 and GLYT2 expressed in *Xenopus* oocytes did not find evidence for oligomerization of these two glycine transporters in the cell surface, although the existence of intracellular oligomers was reported [32]. Additionally, biochemical studies using purified GLYT2 revealed that this protein exists as a monomer in the pig brain [33]. Since the members of the NSS family seem to be subjected to similar trafficking mechanisms, the existence of two exceptions, like GLYT1 and GLYT2, brings into question the influence of oligomerization on specific NSS trafficking. Alternatively, it is possible that oligomers of glycine transporter are very labile and readily disrupted, making their detection difficult through standard biochemical analysis.

In this study we have studied the export of GLYT1 from the ER, showing the conservation of the export mechanisms along the NSS family. Through a mutational

analysis, we have identified an ER export signal in the C-terminus of GLYT1. This signal might be involved in the recruitment of the COPII component Sec24D. In addition, by using FRET microscopy in living cells, we show that GLYT1 can form oligomers along the trafficking pathway that it follows to the plasma membrane, similarly to that described for other members of this transporter family.

EXPERIMENTAL

Materials

[^{3}H]Glycine, Glutathione Sepharose 4B, the pGEX-5x plasmid, protein standards for sodium dodecyl sulfate-polyacrylamide gel electrophoresis (SDS-PAGE Rainbow markers) and ECL western blotting detection reagents were all obtained from Amersham-Pharmacia (Buckinghamshire, U.K.). The Lipofectamine-PLUS, lipofectamine 2000 and the pCDNA3 plasmid were purchased from Invitrogen (Carlsbad, CA), whereas phenylmethanesulfonyl fluoride (PMSF), the Expand High Fidelity PCR system (Taq polymerase) and all restriction enzymes were from Roche (Mannheim, Germany). The QuickChange site-directed mutagenesis kit was from Stratagene Cloning Systems (La Joya, CA). Nitrocellulose sheets were obtained from BioRad (Richmond, CA) and fetal calf serum was supplied by Gibco (Paisley, Scotland). The rabbit anti-calnexin antiserum was from Stressgen bioreagents (Victoria, Canada) while the goat anti-rabbit and goat anti-mouse coupled to Alexa Fluor 488 or Alexa Fluor 555 were from Molecular Probes (Eugene, OR). Vectashield was obtained from Vector (Burlingame, CA) and the reagents Disuccinimidyl suberate (DSS), Bis-(sulfo-succinimidyl) suberate (BS^3) and EZ-linkTM sulfo-NHS-SS-biotin were from Pierce (Rockford, IL). The pGEM-T easy cloning vector was purchased from Promega (Madison, WI) and the oligonucleotides used were synthesized by Isogen (Utrech, NL). All other chemicals were obtained from Sigma Chemical Co. (St. Louis, MO). The CyPetm and YPetm cDNAs, optimized FRET versions of Cyan and Yellow fluorescent proteins, respectively, were a generous gift from Dr. Patrick Daugherty.

Cell growth and transfections

COS 7 and MDCK cells (American Type Culture Collection) were grown at 37°C and 5% CO_2 in high glucose Dulbecco's modified Eagle's medium supplemented with 10% fetal bovine serum. Transient expression in COS 7 or MDCK cells was carried out using Lipofectamine Plus or Lipofectamine 2000, respectively, following the procedures indicated by the supplier. Cells were incubated for 48 h at 37°C and then used for immunofluorescence, biochemical and/or transport assays.

Plasmid constructs

The various GLYT1 mutants used in this study were prepared using the rat GLYT1b in pCDNA3 as a template (derived from the rb20 clone and obtained from Dr. Weinshank) and the QuickChange site-directed mutagenesis kit, according to the manufacturer's instructions. The construct GLYT2Δct was generated by PCR inserting a stop codon at residue 748 of the rat GLYT2 sequence in the reverse primer. Restriction sites for *Hind*III and *Bgl*II were introduced in the forward and reverse primer, respectively and the PCR fragment was cloned into the *Hind*III / *Bam*HI sites of pCDNA3. The GLYT2-GLYT1ct chimera was made by PCR in two steps. First, the sequence corresponding to residues 1-747 of GLYT2 was amplified and cloned as indicated for GLYT2Δct (avoiding the stop codon in the reverse primer), creating the GLYT2-1 / 147 pCDNA3 construct. Subsequently, the sequence corresponding to residues 565 to 638 of GLYT1b was amplified with primers containing restrictions sites for *Bam*HI in the forward primer and for *Xba*I in the reverse primer. The fragment was cloned into the *Bgl*II / *Xba*I digested GLYT2-1/147 pCDNA3. The VSVG-GLYT1ct chimera was also made in two steps. First, the sequence encoding residues 1-498 was amplified by PCR with primers containing restriction sites for *Hind*III and *Bam*HI, and it was then cloned into the equivalent sites of pCDNA3. The GLYT1ct tail was then cloned into the *Bam*HI / *Xba*I sites of this construct, maintaining the correct reading frame. GST-GLYT1Ct was also cloned using PCR into pGEX-5x as described previously [3]. To insert the YFP or CFP tags into these constructs, cDNAs for the fluorescent proteins were amplified by PCR using pYPet-His or pCyPet-His as the template [34]. The forward primer was GCGCGGATCCACCATGGTGAGCAAAGGCGAAGAG and while for CyPetm the reverse primer was GCGCGAATTCTTATTTGTACAGTTCGTCCATGCC, the reverse sequence for YPetm was GCGCGAATTCTTATTTGTACAATTCATTCATCCCTC. The PCR products were then cloned into the *Bam*HI / *Eco*RI sites of pCDNA3. Full length GLYT1 was amplified to eliminate the stop codon and cloned in front of the fluorescent proteins (*Hind*III / *Bam*HI) to create the chimeras GLYT1-YFP and GLYT1-CFP in pCDNA3.

Solubilization and reconstitution in proteoliposomes

Transfected cells from one 10-cm diameter dish were used for each reconstitution experiment. Cells were scraped, collected by centrifugation, and the protein concentration

adjusted to 5-10 mg/ml with phosphate-buffered saline (PBS: 137 mM NaCl; 2.7 mM KCl; 4.3 mM $Na_2HPO_4 \cdot 7H_2O$; 1.4 mM KH_2PO_4; pH 7.3). Cells were solubilized in sodium cholate at a 1:1 detergent / protein ratio. After 10 min on ice, solubilized proteins were reconstituted with asolectin / brain lipids [33], and proteoliposomes were maintained on ice until use.

Transport assays

[^{3}H]Glycine transport in transfected cells or in proteoliposomes was measured as described previously [16, 33].

Protein determination

Protein concentration was determined using the BioRad protein determination kit using bovine serum albumin as the standard.

Cross-linking assays and sucrose gradient velocity centrifugation

Chemical cross-linking was performed using a fraction of the plasma membrane isolated from COS cells or in rat brain synaptosomes isolated as described previously [35]. After incubation at room temperature for 30 min with the cross-linking agents disuccinimidyl suberate or bis-(sulfo-succinimidyl) suberate (BS^3) (5 mM), the reaction was terminated by adding Tris-HCl (pH 7.4) to 50 mM for 15 min. Synaptosomal proteins were solubilized by incubation in RIPA buffer (150 mM NaCl, 2 mM EDTA, 50 mM Tris-HCl pH 8.0, 0.3% SDS, 1% NP40, 0.5% deoxycholate) for 30 min at 4°C. The samples were centrifuged at 100,000 x *g* for 30 min to remove insoluble material, and then layered onto a 10 ml 1-15% sucrose gradient on the top of a 1.0-ml 25% sucrose cushion. The gradient was centrifuged using a SW40.1 rotor in an ultracentrifuge (Beckman Instrument, Inc., Palo Alto, CA) for 16 h at 150,000 x *g*. After centrifugation, samples were collected from the bottom of the tube in 0.5 ml fractions. Proteins were then precipitated with tricloroacetic acid, and resuspended in 100 µl of loading buffer. A sample of 30 µl was analyzed by SDS-PAGE and immunoblotting.

Pull-down assays

COS cells were transfected with an expression vector for *myc*Sec24D and two days later, cells were solubilized in ice-cold lysis buffer (150 mM NaCl, 2 mM EDTA, 50 mM Tris-HCl pH 8.0, 0.1% SDS, 1% NP40, 0.5% deoxycholate) for 30 min at 4°C. The

solubilized material was centrifuged at 14,000 rpm for 20 min, and the supernatant was precleared with 100 µl of a 50% (v/v) glutathione-sepharose bead suspension for 1 h at 4°C with constant rotation. After preclearing, the supernatants were transferred to a clean tube containing glutathione S-transferase (GST), GST-GLYT1ct, or the mutated fusion protein GST-GLYT1ctR575A coupled to glutathione-sepharose, and incubated for 1 h at RT with constant rotation. Subsequently, the beads were washed twice with ice-cold lysis buffer and three times with PBS. Bound proteins were eluted with 10 mM glutathione in 50 mM Tris-HCl, pH 8.0. Finally, 50 µl of SDS-PAGE sample buffer was added to each sample and proteins were resolved by SDS-PAGE on 10% gels, blotted and probed as indicated above using a primary antibody that recognized the 6xHis tag.

Cell Surface Biotinylation

Cells were plated at 50% confluence on 60 mm cell culture plates and transfected as indicated above. After two days, cell surface proteins were labeled having first washed the cells with ice-cold PBS. The cells were then incubated for 20 min at 4ºC in a 1 ml solution containing the non-permeable sulfo-NHS-SS-Biotin reagent (1 mg / ml in PBS). The cells were washed with 2 ml of PBS plus 100 mM lysine for 20 min to quench the reagent. After three additional washes with PBS, the cells were lysed with 1 ml of lysis buffer (150 mM NaCl, 5 mM EDTA, 50 mM Hepes-Tris, 0.25% deoxycholate, 1% Triton X-100, 0.1% SDS, pH 7.4) for 30 min, and the lysate was cleared by centrifugation at 14,000 x g for 10 min. The biotinylated proteins were finally recovered by incubating the cleared lysate for 2 h at RT with streptavidin-agarose beads. After three washes of the beads with 1 ml of lysis buffer, the protein bound to the beads was eluted in 2x Laemmli sample buffer, separated by SDS electrophoresis, and immunoblotted. Biotinylated GLYT1 was visualized with anti-GLYT1 antiserum.

Electrophoresis and blotting

SDS-PAGE was performed in 6% polyacrylamide gels in the presence of 2-mercaptoethanol. Samples from cross-linking experiments were resolved in gradient polyacrylamide gels (4 - 7.5% gels). After electrophoresis, the protein samples were transferred to a nitrocellulose membrane in a semidry electroblotting system at 1.2 mA / cm^2 for 2 h (LKB) and using transfer buffer containing 192 mM glycine and 25 mM Tris-HCl, pH 8.3. Non-specific binding to the membrane was blocked by incubating the

filter with 5% non-fat milk protein in 10 mM Tris-HCl, pH 7.5, 150 mM NaCl for 4 h at 25ºC. The blot was then probed (overnight at 4ºC) with the diluted primary antibody which after washing, was visualized using an anti-rabbit or anti-mouse IgG peroxidase linked secondary antibody. The labeled bands were visualized by ECL and quantified by densitometry (Molecular Dynamics Image Quant v. 3.0).

Immunofluorescence in cultured cells

MDCK cells grown on poly-L-lysine treated glass coverslips were transfected with the corresponding expression vectors using lipofectamine-2000 according to the manufacturers' instructions. Two days later, the cells were rinsed with PBS and fixed for 20 min with 4% paraformaldehyde in PBS. After washing with PBS, the cells were permeabilized and blocked at room temperature for 1 h in PBS containing 1% BSA and 0.02% digitonin. The cells were incubated overnight at 4ºC with anti-GLYT1 [3] in PBS containing 0.1% BSA and 0.02% digitonin. After three washes with PBS, the cells were then incubated with the goat anti-rabbit secondary antibodies conjugated to Alexa 488 (1:250) for 1 h at room temperature. Finally, the cells were washed exhaustively with PBS and the coverslips mounted in Vectashield. The staining was visualized and the images were captured on a confocal microradiance BioRad (Richmond, CA) coupled to an Axioscop2 microscope (Carl Zeiss, Jena, Germany) or in the FRET microscope described below.

FRET Microscopy

FRET efficiency between CyPetm and YPetm fused to GLYT1 was measured in live cells plated on glass bottom culture dishes by sensitized emission, 24 - 48h after transfection. An Axiovert 200M (Zeiss) inverted microscope equipped with Atto-Arc 2 (HBO 100W) epifluorescence illumination, excitation and emission filter wheels (Lambda 10-2, Sutter) and a Ropper Scientific CoolSnap FX monochrome camera was used. Microscope control, image acquisition and processing were achieved using Metamorph 6.2.6 (Universal Imaging). Donor, acceptor and FRET images were acquired sequentially (200 msec exposure, bin 2) with a PlanApo 63X oil-immersion objective (1.4 NA) using a fixed polychroic mirror (86002v2bs, Chroma Technology Corp), the excitation filters (CFP: S430 / 25x, and YFP: S500 / 20x) and the emission filters (CFP: S470 / 30 and YFP: S535 / 30). After background subtraction and shade correction, images were registered using Metamorph. FRET efficiency analysis was

performed using ImageJ software [36] and the PixFret plugin [37]. In all FRET experiments, positive and negative FRET controls were analyzed after transfection of a CFP-YFP tandem (positive control) or cotransfection of CyPetm and YPetm or cotransfection of CyPetmEAAT2 and YPetmGLYT1 (negative controls). Bleed-through coefficients were calculated using fret/donor or fret/acceptor image stacks captured from cells expressing only the donor or acceptor, respectively. Coefficients were averaged from 20 separate stacks for each experiment. Typically, donor bleed through in the FRET channel averaged 38% and acceptor cross-excitation in the FRET channel averaged 4-5%. The PixFRET plugin renders pixel by pixel FRET efficiency values (expressed as %) and typical images are shown. For calculations and statistical evaluation, mean values of intensity histograms constructed from FRET efficiency images were averaged. A minimum of 40 different cell stacks were taken in each experiment.

RESULTS

The C-terminal domain of GLYT1 contains trafficking sequences transplantable to another neurotransmitter transporter

Previous studies of GLYT1 deletion mutants revealed the importance of residues located in the cytoplasmic C-terminus for the correct trafficking of the transporter from the endoplasmic reticulum to the plasma membrane [13, 15]. To investigate whether the domain corresponding to residues 565 to 638 of GLYT1b (GLYT1ct) contains sufficient information to promote ER export, acting as an autonomous export signal, we analyzed the capacity of GLYT1ct to promote ER exit when placed in the context of other proteins (see the scheme in Figure 1J). Like GLYT1, deletion of the C-terminus (residues 748 to 799) of the related GLYT2 glycine transporter produced a protein (GLYT2Δct) incapable of reaching the plasma membrane of transfected MDCK cells (Figure 1A-C). This contrasted with the capacity of YFP-EAAT2 to reach the plasma membrane, a glutamate transporter that was cotransfected with GLYT2Δct to control for the integrity of the ER export pathway and to clearly identify the membrane compartment. A chimera in which the C-terminus of GLYT2 was replaced with GLYT1ct (GLYT2-GLYT1ct) was properly inserted in the plasma membrane and co-localized with YFP-EAAT2 in most of the transfected cells (Figure 1D-F). A quantitative estimation of the amount of these constructs that reached the plasma membrane was obtained by measuring their glycine uptake capability (Figure 1K). While glycine uptake measured in cells transfected with the construct GLYT2Δct was only 2% of that observed with GLYT2wt, the uptake after transfection of the chimera GLYT2-GLYT1ct was 53% of the wild type value (Figure 1K). Differently to the GLYT2-GLYT1ct construct, a chimera containing residues 1 to 498 of the vesicular stomatitis virus glycoprotein VSVG plus GLYT1ct was unable to exit the ER (Figure 1G-I). This is entirely consistent with previous reports that studied the traffic of VSVG and that showed that a C-terminal diacidic motif (residues 500-511) of wild type VSVG controls its trafficking to the plasma membrane [38]. This signal was absent in the VSVG-GLYT1ct chimera and could not be substituted, at a functional level, by the addition of the GLYT1ct tail. Thus, the export signal of GLYT1ct seems to only operate in the context of related proteins, suggesting that it needs additional export determinants provided by upstream sequences not contained in the transplanted peptide.

Identification of the intracellular residues important for GLYT1 exit from the ER

The capacity of the GLYT1ct export signal to substitute for that of GLYT2ct indicates that it is evolutionarily conserved. To more precisely identify residues involved in the exit of GLYT1 from the ER, we compared the amino acidic sequence of the GLYT1ct with that of related NSS family transporters. In this gene family, only five amino acids are highly conserved in this particular region of the transporter: G569, L572, R575, L576 and P582 (Figure 2A). Additionally, residue D585 is conserved in most NSS transporters although in BTGT, TAUT and SERT non-conservative substitutions can be found (proline or serine) (Figure 2A). We substituted residues G569, R575, L576, P582 and D585 (arrows in Figure 2A) using site directed mutagenesis, introducing either alanine, or other conserved or non-conserved residues. Subsequently, the function of these mutants was analyzed in transport assays in transiently transfected COS cells (Figure 2B). Two of these mutated residues (R575 and L576) did not admit the alanine substitution and produced inactive transporters. Moreover, while conservative substitutions at these sites did yield active transporters (R575K and R576I, respectively), non-conservative substitutions (R575D and L576D, respectively) abolished the capacity to transport glycine. In addition, mutations in position D585 had a drastic effect on the transporter activity since mutant D585A lost about 80 percent of the transport capability, and its mutation to arginine reduced the activity by a 75 percent. Recently, it was shown that the equivalent residues to R575 and L576 in the related GABA transporter GAT1 play an essential role in the traffic of this transporter to the plasma membrane [19]. However, the equivalent residue to D585 was not investigated in that study. Thus, we analyzed how mutations in this position might affect the transport of substrates through GAT1 (residue D576) and the glycine transporter GLYT2 (residue D759). Mutations in GAT1 had a small effect on the GABA uptake (reduced by 7% in GAT1-D576A and 15% in GAT1-D576R). However, this residue was more important for GLYT2, where glycine uptake was reduced by 39 and 67% in mutants GLYT2-D759A and GLYT2-D759R, respectively (Figure 2C).

The G569A and P582A mutants of GLYT1 transported glycine with an efficiency similar to that of wild-type GLYT1, suggesting that these positions are not crucial for GLYT1 function (Figure 2B). The conserved L572 residue has already been studied in a previous publication and was therefore not analyzed further. Indeed, the L572A mutant was functional although it was missorted in polarized cells [13].

The inactive mutants R575 and R576 and the partially active D585A are retained in the endoplasmic reticulum

To elucidate why some of these mutants displayed impaired activity, we analyzed their subcellular distribution by immunofluorescence and through biotinylation assays. Accordingly, we found that the inactive mutants R575A (Figure 3B), R575D (Figure 3C) and L576A (Figure 3E) were retained in the intracellular compartment, whereas the active mutants R575K (Figure 3D), L576I (Figure 3F), G569A (Figure 3G) and P582A (Figure 3H) displayed a similar subcellular distribution to that of the wild type transporter (Figure 3A), with a clear labeling of the plasma membrane. The partially active mutant D585A was largely retained in the intracellular compartment, but a weak staining of the plasma membrane was appreciated in some cells (Figure 3I). These results were concordant with those observed in biochemical assays in which membrane proteins were biotinylated with the membrane impermeable reagent sulfo-NHS-SS-biotin. When the biotinylated proteins were recovered using streptavidin agarose beads and analyzed by immunoblotting, the inactive mutants (R575 and L576) were clearly not accessible to biotinylation due to their intracellular retention. In contrast, the active mutants were biotinylated, while mutant D585A that has a low transport capability was weakly accessible to biotinylation (Figure 4A). As reported previously, two GLYT1wt bands are detected in immunoblots corresponding to the total cell lysate [39]. The faster migrating form corresponds to a partially glycosylated transporter that resides in the endoplasmic reticulum, while the slower one corresponds to the fully glycosylated GLYT1, and is accessible to biotinylation. As expected, mutants retained in the intracellular compartment were only detected as a single, faster migrating band, whereas both bands could be identified of the mutants that progressed to the plasma membrane. It has to be noted the relatively low protein level detected in the intracellularly retained mutants that, in part, might be due to the tendency to aggregate of these forms of the protein yielding adducts that were not properly resolved in SDS-PAGE. Additionally, forms of the protein retained in the intracellular compartment might be rapidly degraded. To rule out the possibility that defective membrane targeting was due to mutant GLYT1 misfolding, glycine transport was assayed in reconstituted proteoliposomes obtained from COS cells transfected with mutants or wild type GLYT1. After their reconstitution into proteoliposomes, the mutants R575A, R575D and L576A all displayed greater percentage of activity than that measured in native COS cells (Figure 4B), indicating that the retained mutants were intrinsically capable of mediating glycine uptake. Moreover a kinetics analysis of the glycine uptake by

these reconstituted mutants revealed no significative changes in the Km of the mutants in comparison with the wild type transporter (Km values were 31 ± 5 µM for R575A, 24 ± 4 µM for R575D, 28 ± 5 µM for L576A and 18 ± 3 µM for GLYT1wt). Hence, we could consider that these mutants were properly folded.

Since the R575A and L576A and D585A largely colocalized with the ER marker calnexin, they were clearly retained in the endoplasmic reticulum (Figure 5A-C and the supplementary Figure 1). The staining of the wild type form was clearly dissociated from calnexin in most of the cells, since it was mainly detected in the plasma membrane (Figure 5D-F). However, occasionally, some cells overexpressing GLYT1wt also showed intracellular localization of GLYT1wt which colocalized with calnexin (data not shown). The importance of the $R^{575}L^{576}(X)_8D^{585}$ motif for ER export was reinforced by the intracellular retention of the R575A mutation in the context of the GLYT2-GLYT1ct chimera (Figure 5J-L), in contrast to the chimera that contained the wild type form of GLYT1ct (Figure 5G-I, and Figure 1D-F). A GLYT2-GLYT1ct chimera containing mutations L576A or D585A was also retained in the ER (data not shown).

Recently, the dibasic [RK](X)[RK] motif has been proposed to be involved in ER export of the Golgi resident glycosyltransferases [40]. Because residue 577 of GLYT1 is a lysine, the sequence $R^{575}L^{576}K^{577}$ could fit into this class of export signal. However, the K577A mutant was exported to the plasma membrane and transported glycine as efficiently as GLYT1wt (data not shown), ruling out this possibility. Similarly, the $D^{568}G^{569}D^{570}$ sequence of GLYT1ct could also be considered as such a diacidic ER export motif (see Figure 2A) [38]. However, again the D570A mutant was delivered normally to the plasma membrane (data not shown), equally ruling out the participation of this motif in ER export of GLYT1.

Sec24 interacts with the $RL(X)_8D$ motif of GLYT1ct

ER export involves recruitment of cargo proteins to ER-derived vesicles by the coat protein complex II (COPII). The first step in the capture of the cargo seems to be accomplished by the coordinate binding of the COPII components Sar1 GTPase, the Sec23-24 complex, followed by the Sec13-Sec31 complex. Recently, the homologous RL motif of the GABA transporters was shown to interact with Sec24D [19]. Thus, to investigate the possible involvement of the $RL(X)_8D$ motif in binding to COPII we analyzed the capacity of GST fusion proteins containing the wild-type GLYT1ct (GST-G1ct in Figure 6) or with mutations in the R575, L576 or D585 positions (GST-

G1ctR575A, GST-G1ctL576A and GST-G1ctD585A) to pull-down a *myc*-tagged form of Sec24D (*myc*-Sec24D) expressed in transfected COS cells. While some non-specific *myc*-Sec24D binding to control GST beads was observed (Figure 6A), there was a clear increase in the amount of *myc*-Sec24D that was precipitated by GST-G1ct but not by the fusion protein mutated at position 575 or 576 of GLYT1ct (GST-G1ctR575A and GST-G1ctL576A). A quantitative estimation of the binding capability was obtained by densitometric analysis of immunoblots (Figure 6B). Although mutant GST-G1ctD585A conserved some capability to pull-down *myc*-Sec24D (3.8 times over the GST control), this was clearly lower than GST-G1ct (6.4 times over the GST control), while the binding to GST-G1ctR575A and GST-G1ctL576A was similar to that of GST (Figure 6A,B). Hence, the $RL(X)_8D$ motif appears to participate in the interaction with the component of COPII complex Sec24D.

Trafficking of R575 and L576 mutants can be partially rescued by coexpression with wild-type GLYT1

Immunofluorescence assays indicated that when the inactive R575A or L576 mutants were coexpressed in MDCK cells with wild-type GLYT1, a proportion of the mutant protein was able to reach the plasma membrane (Figure 7A-C). In these experiments, the GLYT1 constructs were either tagged at the N-terminus with green fluorescent protein (GFP) or with the HA epitope, and they were then visualized by double immunofluorescence. Control experiments revealed that the inclusion of these tags into GLYT1wt or mutants had no functional consequences either on transport or on the targeting processes (data not shown). However, when GFP tagged forms of the mutant R575A (G-R575A) were coexpressed with HA-tagged GLYT1wt (HA-GLYT1wt), the mutant protein was now detected in the plasma membrane of cells with a low expression level of the mutant (Figure 7D-F). The recruitment to the plasma membrane of the R575A mutant did not occur in a control experiment performed by coexpressing G-R575A with the glutamate transporter (HA-EAAT2) (Figure 7G-I). Similar observations were performed for L576A mutant (Figure 7J-O)

GLYT1 oligomer formation

These immunocytochemical experiments suggested the existence of an interaction between the mutated forms of the transporter (R575A and L576A) and the native form of GLYT1 along the biosynthetic pathway, possibly involving oligomerization. Indeed, other

members of the NSS transporter family are known to form oligomers, and an oligomerization step has been suggested to be part of the endoplasmic reticulum quality control mechanism for these closely related transporters. Nevertheless, previous experiments performed in *Xenopus* oocytes with cross-linker reagents failed to demonstrate oligomerization of GLYT1 [32]. In our hands, chemical cross-linkers favored the formation of high molecular weight aggregates containing the transporter in transfected COS cells (data not shown), but the interpretation of these experiments was complicated by the tendency of GLYT1 to aggregate unspecifically during the solubilization procedures in transfected cells. Unspecific aggregation was not observed in rat brain membranes and, then, we studied the possible existence of GLYT1 oligomers in a preparation of synaptosomes. Putative oligomers were stabilized by treating the synaptosomal fraction with cross-linker reagents. Two reagents were used, the membrane permeable bifunctional lysine cross-linker DSS or its non-permeable analog BS^3 (sulfo-DSS) [41]. The cross-linked adducts were solubilized and resolved by sucrose gradient velocity sedimentation, followed by SDS-PAGE and immunoblotting analysis of the fractions obtained from the sucrose gradient (Figure 8A-B). Immunoreactivity for GLYT1 was detected in several fractions, with most of the protein migrating as a monomer with both reagents. The peak of this form of the protein was found in fraction 5, which corresponded to 3.3% sucrose (Figure 8). Densitometric analysis of the immunoblots indicated that 88.0 ± 2.3 (n = 3) of the total protein treated with DSS that had been loaded in the gradient migrated as a monomer in SDS-PAGE, while in samples reacted with BS^3, the monomer represented 92.8 ± 2.5 (n = 3) of the total protein (Figure 8C). A form of GLYT1 with the electrophoretic mobility expected for a dimer had a peak around the fraction 7 (4.7% sucrose) and represented 4.9 ± 0.4 and 4.5 ± 0.4 of the total protein in the presence of DSS or BS^3, respectively (Figure 8C). Since it was equally accessible to both reagents it seems to be located mainly in the cell surface. Another form of GLYT1, with the mobility expected for a tetramer, had a peak around the fraction 8 (5.3% sucrose). In this case the amount of adduct measured in the presence of the permeable reagent DSS was significantly higher than that observed in the presence of BS^3, (7.1 ± 0.6 % and 2.7 ± 0.3 %, $P < 0.01$), suggesting that tetrameric arrangements of GLYT1 are more abundant in the intracellular compartment (Figure 8C). Additional adducts of higher density were also resolved in the sucrose gradients, but their electrophoretic mobility could not be measured with precision. Although the flotation characteristics and the electrophoretic mobility of the different GLYT1 adducts are compatible with the oligomerization of this protein, these

data obtained in synapsotomes cannot rule out the possibility that these complexes would be formed by GLYT1 and other interacting proteins instead of GLYT1 protomers. Thus, to avoid the complications of the use of cross-linkers and to investigate the possibility that labile GLYT1 oligomers might also form along their biosynthetic pathway, we decided to use also a less invasive technique by measuring the efficiency of Fluorescence Resonance Energy Transfer (FRET) between GLYT1wt with CyPetm or Ypetm fused to its C-terminus. CyPetm and YPetm are optimized FRET versions of cyan and yellow fluorescent proteins [34]. We used a wide-field microscope to measure FRET as an increase in acceptor fluorescence resulting from donor excitation (i.e. sensitized emission FRET). Images collected in the FRET channel were corrected for CFP and YFP spectral bleed-through and normalized for expression levels (NFRET), as indicated in the Materials and Methods section. Figure 9A-C provide representative images showing subcellular distribution of NFRET in COS cells co-transfected with GLYT1-CyPetm plus GLYT1-YPetm. Normalized FRET values are represented in a pseudocolor scale, and clearly reveals the existence of FRET in the plasma membrane of transfected cells (Figure 9A,B). In those cells were ER forms of GLYT1 were observable, FRET was also appreciated in the intracellular compartment (Figure 9C). To perform the statistical analysis presented in Figure 9D, the mean values of the intensity histograms, constructed from the FRET efficiency images recorded over the whole surface delimited by the cell contour, were averaged and presented as a bar histogram. These values were compared with a negative control obtained by the co-expression of CyPetm and YPetm, and a positive control with a CFP-YFP tandem construct. Cells transfected with GLYT1-CyPetm plus GLYT1-YPetm showed a FRET efficiency significantly higher than that of the negative control (15.52 ± 1.30% for GlyT1, versus 2.73 ± 0.63% for the negative CyPetm + YPetm control and 48.21 ± 1.85% for the positive control (CFP-YFP), $P < 0.001$, paired t-test with negative control). The FRET efficiency between the pair GLYT1-CyPetm and GLYT1-YPetm was also higher than that measured using as a donor the CFP-tagged form of the glutamate transporter EAAT2 (EAAT2-CyPetm) and GLYT1-YPetm as the acceptor (0.39 ± 0.15%) (Figure 9D), despite that both proteins colocalize in the plasma membrane, indicating that the measured FRET was not due to unspecific aggregation of overexpressed plasma membrane proteins.

DISCUSSION

The precise localization of neurotransmitter transporters in specific compartments of the neuronal and perhaps the glial plasma membrane seems to be critical for the correct function of these proteins. One of the first steps in the correct targeting of the transporter is the exit from the ER. In those NSS transporters so far analyzed this involves both the oligomerization of the transporter and the interaction of specific residues of the C-terminus with the RE export machinery [15]. Previous evidence suggested that the glycine transporter GLYT1 might use an ER export mechanism that could differ significantly from that used by other members of the NSS family, since it was reported the absence of oligomerization. Consequently, in the present work we investigated the mechanisms of exit of the GLYT1 from the ER. However, our findings support a mechanism of ER export of GLYT1 similar to that of other NSS transporters. Here, we have identified the $R^{575}L^{576}(X_8)D^{585}$ motif, which is evolutionarily conserved across the NSS transporter family and that is necessary for targeting GLYT1 to the plasma membrane. The RL moiety of the motif also mediates the ER export of the GABA transporter GAT1 [21]. Moreover, RL operates in GAT1 by a similar mechanism since it also mediated the interaction of the transporter with the component of the COPII complex Sec24D (see below). Consistently with the evolutionary conservation of this sequence, mutations of lysine-590 of the dopamine transporter (DAT), equivalent to R575 in GLYT1, also provoked the retention of DAT in the ER [20]. Evolutionary conservation of D585 is less strict. Nevertheless, it is required for efficient expression not only of GLYT1, but also for GLYT2 (D759) (this report) and for DAT (K600) [20]. It seems to play a minor role for GAT1 expression. The $RL(X_8)D$ motif of GLYT1 differs from the three types of ER export motifs previously reported (the diacidic, the dihydrophobic and the dibasic motifs) [42]. The diacidic motif is required for efficient export of the VSVG protein in mammalian cells [38] and it has also been found in Kir2.1 potassium channels, among other proteins [43]. Interestingly, a diacidic motif that is not conserved in the NSS gene family can be found in GLYT1ct (residues $D^{568}G^{569}D^{570}$, Figure 2A). However, this motif does not seem to regulate ER export of GLYT1 since the D570A mutant reached the plasma membrane (data not shown). Moreover, this sequence was unable to replace the endogenous diacidic motif of the viral protein VSVG, despite its inclusion in the transplanted fragment of GLYT1, suggesting that it is not in the appropriate context to promote ER export. Another RE export motif is the dihydrophobic motif that is used by proteins like ERGIC-53 or p24 [44, 45]. The carboxy

terminus of GLYT1 also contains two dileucine motifs that could be considered to fit into the dihydrophobic class of ER export motif. However, previous studies from our laboratory ruled out this possibility since transporters with mutations in this motif reached the plasma membrane, although their distribution was altered in polarized MDCK cells. Accordingly, this motif might act in sorting GLYT1 to the basolateral surface in the trans-Golgi network. ER export of glycosyltransferases is dependent on a dibasic motif in their cytoplasmic tails which fits to the consensus sequence [RK](X)[RK] [40]. Since a lysine (K577) follows the RL half of the $R^{575}L^{576}(X_8)D^{585}$ motif, this GLYT1 sequence could be a variant of the dibasic motif. However, it appears to behave differently since the K577A mutant was efficiently exported to the plasma membrane. Moreover, although this second lysine residue is present in GLYT2, in the GABA transporter GAT2, and in the taurine transporter TAUT, it is not conserved in other transporters of the NSS family (Figure 2A).

Surprisingly, mutations at two other evolutionary conserved positions of GLYT1, G569 and P582, produced a transporter that underwent apparently normal trafficking and that display normal transport activity. Indeed, the G585A mutation in DAT, the equivalent to G569 in GLYT1, produced a dramatic effect on DAT export from the ER [20]. It is possible that the mutation of these residues to alanine is not sufficiently deleterious to alter the properties of GLYT1. Thus, less conservative mutations would be necessary to evaluate the real importance of these two strictly conserved residues.

The three known ER export motifs interact with components of the COPII complex so as to incorporate into COPII vesicles. Our data support a similar interaction between the $RL(X_8)D$ motif of GLYT1 and Sec24D of the COPII complex. However, this interaction seems not to be sufficient to promote ER export of GLYT1 since it was not transplantable to an unrelated protein like VSVG. These not yet identified additional ER export signals seem to be present in the related transporter GLYT2. Indeed, other export motifs characterized to date are not readily transferred to other proteins, suggesting that multiple determinants are commonly involved for the recruitment of many proteins into COPII vesicles.

The effects of mutations in the $RL(X_8)D$ motif were partially rescued by coexpression of mutated proteins with the native form of the transporter, GLYT1wt. This observation suggested that oligomers of GLYT1 form along the secretory pathway, with the GLYT1wt providing the mutant forms with the necessary signal for ER export. Other NSS transporters like GAT1, DAT, NET or SERT, have been shown to be capable of forming oligomers and this might be related with their trafficking to the plasma membrane [review

15]. However, a previous report failed to identify GLYT1 and GLYT2 oligomers in the cell surface of *Xenopus* oocytes that had been injected with the mRNA encoding these transporters [32], and monomers were also detected in another study on the hydrodynamic properties of a glycine transporter purified from pig brainstem [33]. The fact that two member of the NSS family might be incapable of undergoing oligomerization raised questions about the real importance of oligomerization in the physiology of this family of transporters. Nevertheless, the study in *Xenopus* oocytes had detected intracellular forms of GLYT1 and GLYT2 with an electrophoretic mobility that was consistent with the existence of oligomers [32]. Thus, we reevaluated the capacity of GLYT1 to form oligomers in the rat brain by using chemical crosslinkers and in transfected living cells by using FRET microscopy. Results obtained by using these two approaches are compatible with the formation of GLYT1 oligomers. While FRET microscopy indicates that GLYT1 is able to form oligomers both in the cell surface and in the intracellular compartment, the crosslinking experiments in native rat brain membranes suggest that such complexes appear to exist also *in vivo,* although in limited amounts (about 12% of the total GLYT1). The relatively low level of GLYT1 oligomers in these native membranes or their absence in the cell surface of *Xenopus* oocytes indicates that oligomerization may not be an essential determinant for substrate transport but rather that oligomerization influences trafficking. The preferential localization of tetrameric arrangements in the intracellular compartment that we detected with the use of differentially permeable cross-linker reagents, and the referred oligomeric intracellular forms detected in *Xenopus* oocytes [32] would be compatible with this idea. The identification of GLYT1 oligomers indicates that oligomerization is, indeed, a general feature of NSS transporters, although the biological significance of their formation remains unclear. Our data are compatible with the hypothesis that oligomerization might bring together several ER COPII binding motifs, thereby increasing the efficiency of ER export of this family of transporters [15, 19].

GLYT1 is a transporter enriched in glial cells in the glycinergic areas of the nervous system as well as in glutamatergic neurons, where it is strategically placed close to NMDA receptors, thereby regulating both glycinergic and glutamatergic activity in the nervous system. GLYT1 is exported from the ER through a multistep process that involves glycosylation [39], oligomerization and an interaction with the COPII complex through a specific and evolutionarily conserved motif present in the carboxyl tail of the protein. After escaping this stringent quality control of the ER, GLYT1 is sorted in the Golgi apparatus and delivered to the plasma membrane, where it is inserted by the exocyst and anchored to

scaffold proteins in the cell surface to regulate extracellular levels of the neuroactive glycine [6, 13, 46].

Acknowledgements

We would like to thank E. Núñez for expert technical help and Carlos Sánchez in the confocal microscopy department of the CBMSO. We also wish to thank Dr. Daugherty for CyPetm and YPetm plasmids and Dr. H. Wong for the *myc*-Sec24D plasmid. This work was supported by grants from the Spanish "Dirección General de Investigación Científica y Técnica" (SAF2005-03185), the "Comunidad Autónoma de Madrid" and by an institutional grant from the "Fundación Ramón Areces".

REFERENCES

1 Kemp, J. A., and Leeson, P. D. (1993) The glycine site of the NMDA receptor-five years on. Trends Pharmacol. Sci. **14,** 20-25

2 Nong, Y., Huang, Y.-Q., Ju, M., Kalla, L. V., Ahmadian, G., Wang, Y. T., and Salter, M. W. (2003) Glycine binding primes NMDA receptor internalization. Nature **422,** 302-307

3 Zafra, F., Aragón, C., Olivares, L., Danbolt, N. C., Giménez, C., and Storm-Mathisen, J. (1995) Glycine transporters are differentially expressed among CNS cells. J. Neurosci. **15,** 3952-3969

4 Gomeza, J., Hülsmann, S., Ohno, K., Eulenburg, V., Szöke, K., Richter, D., and Betz, H. (2003) Inactivation of the glycine transporter 1 gene discloses vital role of glial glycine uptake in glycinergic inhibition. Neuron **40,** 785-796

5 Cubelos, B., Giménez, C., and Zafra, F. (2005) Localization of the GLYT1 glycine transporter at glutamatergic synapses in the rat brain. Cereb. Cortex **15**, 448-459

6 Cubelos, B., González-González, I. M., Giménez, C., and Zafra, F. (2005) The scaffolding protein PSD-95 interacts with the glycine transporter GLYT1 and impairs its internalization. J. Neurochem. **95**, 1047-1058

7 Bergeron, R., Meyer, T. M., Coyle, J. T., and Greene, R. W. (1998) Modulation of N-methyl-D-aspartate receptor function by glycine transport. Proc. Natl. Acad. Sci. U. S. A. **95,** 15730-15734

8 Chen, L., Muhlhauser, M., and Yang, C. R. (2003) Glycine tranporter-1 blockade potentiates NMDA-mediated responses in rat prefrontal cortical neurons in vitro and in vivo. J. Neurophysiol. **89,** 691-703

9. Kinney, G. G., Sur, C., Burno, M., Malorga, P. J., Williams, J. B., Figueroa, D. J., Wittmann, M., Lemaira, W., and Conn, P. J. (2003) The glycine transporter type 1 inhibitor N-[3-(4'-fluorophenyl)-3-(4'-phenylphenoxy)propyl]sarcosine potentiates NMDA receptor-mediated responses in vivo and produces an antipsychotic profile in rodent behaviour. J. Neurosci. **23,** 7586-7591

10 Tsai, G., Ralph-Williams, R. J., Martina, M., Bergeron, R., Berger-Sweeney, J., Dunham, K. S., Jiang, Z., Caine, S. B., and Coyle, J. T. (2004) Gene knockout of glycine transporter 1: characterization of the behavioral phenotype. Proc. Natl. Acad. Sci. U. S. A. **101,** 8485-8490

11 Gabernet, L., Pauly-Evers, M., Schwerdel, C., Lentz, M., Bluethmann, H., Vogt, K., Alberati, D., Mohler, H., and Boison, D. (2005) Enhancement of the NMDA receptor function by reduction of glycine transporter-1 expression. Neurosci. Lett. **373**, 79-84

12 Yee, B. K., Balic, E., SiYee, B. K., Balic, E., Singer, P., Schwerdel, C., Grampp, T., Gabernet, L., Knuesel, I., Benke, D., Feldon, J., Mohler, H., and Boison, D. (2006) Disruption of glycine transporter 1 restricted to forebrain neurons is associated with a procognitive and antipsychotic phenotypic profile. J. Neurosci. **26**, 3169-3181

13 Poyatos, I., Ruberti, F., Martinez-Maza, R., Giménez, C., Dotti, C. G., and Zafra, F. (2000) Polarized distribution of glycine transporter isoforms in epithelial and neuronal cells. Mol. Cell. Neurosci. **15**, 99-111

14 Melikian, H. E. (2004) Neurotransmitter transporter trafficking: endocytosis, recycling, and regulation. Pharmacol. Ther. **104**, 17-27

15 Sitte, H. H., Farhan, H., and Javitch, J. A. (2004) Sodium-Dependent Neurotransmitter Transporters: Oligomerization as a Determinant of Transporter Function and Trafficking. Mol. Interv. **4**, 38-47

16 Olivares, L., Aragón, C., Giménez, C., and Zafra, F. (1994) Carboxyl terminus of the glycine transporter GLYT1 is necessary for correct processing of the protein. J. Biol. Chem. **269**, 28400-28404

17 Torres, G. E., Yao, W. D., Mohn, A. R., Quan, H., Kim, K. M., Levey, A. I., Staudinger, J., and Caron, M. G. (2001) Functional interaction between monoamine plasma membrane transporters and the synaptic PDZ domain-containing protein PICK1. Neuron **30**,121-134

18 Torres, G. E., Carneiro, A., Seamans, K., Fiorentini, C., Sweeney, A., Yao, W. D., and Caron, M. G. (2003) Oligomerization and trafficking of the human dopamine transporter. Mutational analysis identifies critical domains important for the functional expression of the transporter. J. Biol. Chem. **278**, 2731-2739

19 Farhan, H., Korkhov, V. M., Paulitschke, V., Dorostkar, M. M., Scholze, P., Kudlacek, O., Freissmuth, M., and Sitte, H. H. (2004) Two discontinuous segments in the carboxyl terminus are required for membrane targeting of the rat gamma-aminobutyric acid transporter-1 (GAT1). J. Biol. Chem. **279**, 28553-28563

20 Miranda, M., Sorkina, T., Grammatopoulos, T. N., Zawada, W. M., and Sorkin, A. (2004) Multiple molecular determinants in the carboxyl terminus regulate dopamine transporter export from endoplasmic reticulum. J. Biol. Chem. **279**, 30760-30770

21 Farhan, H. Reiterer, V., Korkhov, V. M., Schmid, J. A., Freissmuth, M. and Sitte, H. H. Concentrative Export from the Endoplasmic Reticulum of the {gamma}-Aminobutyric Acid Transporter 1 Requires Binding to SEC24D. J. Biol. Chem. **282** 7679-7689

22 Mellerup, E. T., Plenge, P., and Nielsen, M. (1984) Size determination of binding polymers for [^{3}H]imipramine and [^{3}H]paroxetine in human platelet membranes. Eur. J. Pharmacol. **106**, 411–413

23 Berger, S. P., Farrell, K., Conant, D., Kempner, E. S., and Paul, S. M. (1994) Radiation inactivation studies of the dopamine reuptake transporter protein. Mol. Pharmacol. **46**, 726–731

24 Kilic, F., and Rudnick, G. (2000) Oligomerization of serotonin transporter and its functional consequences. Proc. Natl. Acad. Sci. U. S. A. **97**, 3106–3111

25 Sorkina, T., Doolen, S., Galperin, E., Zahniser, N. R., and Sorkin, A. (2003) Oligomerization of dopamine transporters visualized in living cells by fluorescence resonance energy transfer microscopy. J. Biol. Chem. **278**, 28274–28283

26 Jess, U., Betz, H., and Schloss, P. (1996) The membrane-bound rat serotonin transporter, SERT1, is an oligomeric protein. FEBS Lett. **394**, 44–46

27 Hastrup, H., Karlin, A., and Javitch, J. A. (2001) Symmetrical dimer of the human dopamine transporter revealed by cross-linking Cys-306 at the extracellular end of the sixth transmembrane segment. Proc. Natl. Acad. Sci. U. S. A. **98**, 10055–10060

28 Norgaard-Nielsen, K., Norregaard, L., Hastrup, H., Javitch, J. A., and Gether, U. (2002) Zn(2+) site engineering at the oligomeric interface of the dopamine transporter. FEBS Lett. **524**, 87–91

29 Kitayama, S., Ikeda, T., Mitsuhata, C., Sato, T., Morita, K., and Dohi, T. (1999) Dominant negative isoform of rat norepinephrine transporter produced by alternative RNA splicing. J. Biol. Chem. **274**, 10731–10736

30 Just, H., Sitte, H. H., Schmid, J. A., Freissmuth, M., and Kudlacek, O. (2004) Identification of an additional interaction domain in transmembrane domains 11

and 12 that supports oligomer formation in the human serotonin transporter. J. Biol. Chem. **279**, 6650-6657

31 Schmid, J. A., Scholze, P., Kudlacek, O., Freissmuth, M., Singer, E. A., and Sitte, H. H. (2001) Oligomerization of the human serotonin transporter and of the rat GABA transporter 1 visualized by fluorescence resonance energy transfer microscopy in living cells. J. Biol. Chem. **276**, 3805–3810

32 Horiuchi, M., Nicke, A., Gomeza, J., Aschrafi, A., Schmalzing, G., and Betz, H. (2001) Surface-localized glycine transporters 1 and 2 function as monomeric proteins in Xenopus oocytes. Proc. Natl. Acad. Sci. U. S. A. **98**,1448–1453

33 Lopez-Corcuera B, Alcantara R, Vazquez J, and Aragon C. (1993) Hydrodynamic properties and immunological identification of the sodium- and chloride-coupled glycine transporter. J. Biol. Chem. **268**, 2239-2243

34 Nguyen, A. W., and Daugherty, P. S. (2005) Evolutionary optimization of fluorescent proteins for intracellular FRET. Nat. Biotechnol. **2005**, 355-360

35 Nagy, A., and Delgado-Escueta, A. V. (1984) Rapid preparation of synaptosomes from mammalian brain using nontoxic isoosmotic gradient material (Percoll). J. Neurochem. **43**, 1114-1123

36 Rasband, W. S., in Image J., U. S. National Institutes of Health, Bethesda, Maryland, USA, http://rsb.info.nih.gov/ij/, 1997-2006

37 Feige, J. N., Sage, D., Wahli, W., Desvergne, B., and Gelman, L. (2005) PixFRET, an ImageJ plug-in for FRET calculation that can accommodate variations in spectral bleed-throughs. Microsc. Res. Tech. **68**, 51-58

38 Nishimura, N., and Balch, W. E. (1997) A di-acidic signal required for selective export from the endoplasmic reticulum. Science **277**, 556-558

39 Olivares, L., Aragón, C., Giménez, C., and Zafra, F. (1995) The role of N-glycosylation in the targeting and activity of the GLYT1 glycine transporter. J. Biol. Chem. **270**, 9437-9442

40 Giraudo, C. G., and Maccioni, H. J. (2003) Endoplasmic reticulum export of glycosyltransferases depends on interaction of a cytoplasmic dibasic motif with Sar1. Mol. Biol. Cell. **14**, 3753-3766

41 Staros, J. V., Kotite, N. J., and Cunningham, L. W. (1992) Membrane-impermeant cross-linking reagents for structural and functional analyses of platelet membrane glycoproteins. Methods Enzymol. **215,** 403-124

42 Barlowe, C. (2003) Signals for COPII-dependent export from the ER: what's the ticket out?. Trends Cell. Biol. **13**, 295-300

43 Ma, D., Zerangue, N., Lin, Y. F., Collins, A., Yu, M., Jan, Y. N., and Jan, L. Y. (2001) Role of ER export signals in controlling surface potassium channel numbers. Science **291**, 316-319

44 Nufer, O., Guldbrandsen, S., Degen, M., Kappeler, F., Paccaud, J. P., Tani, K., and Hauri, H. P. (2002) Role of cytoplasmic C-terminal amino acids of membrane proteins in ER export. J. Cell. Sci. **115**, 619-628

45 Dominguez, M., Dejgaard, K., Fullekrug, J., Dahan, S., Fazel, A., Paccaud, J. P., Thomas, D. Y., Bergeron, J. J., and Nilsson, T. (1998) gp25L/emp24/p24 protein family members of the cis-Golgi network bind both COP I and II coatomer. J. Cell. Biol. **140**, 751-765

46 Cubelos, B, Giménez, C., and Zafra, F. (2005) The glycine transporter GLYT1 interacts with Sec3, a component of the exocyst complex. Neuropharmacol. **49**, 935-944

Abbreviations: BSA, bovine serum albumin; CFP, cyan fluorescent protein; GLYT1 and 2, glycine transporter-1 and 2; DAT, dopamine transporter and GAT1, γ-aminobutyric transporter; vGLUT, vesicular glutamate transporter; COP, coatomer coat proteins; VSVG, vesicular stomatitis virus glycoprotein; GST, glutathione-S-Transferase; MESNA, 2-mercaptoethanesulphonic acid; NMDA, N-Methyl-D-Aspartate; NMDAR, NMDA receptor; NSS, sodium and chloride-dependent neurotransmitter transporter; PBS, phosphate-buffered saline; FRET, fluorescence resonance energy transfer; YFP, yellow fluorescent protein.

FIGURE LEGENDS

Figure 1. Localization of chimeras containing the carboxyl terminus of GLYT1
MDCK cells were transiently transfected with YFP-EAAT2 as well as the truncated form of GLYT2 (GLYT2Δct) (**A-C**), the chimera GLYT2-GLYT1ct (**D-F**), or the chimera VSVG-GLYT1ct (G-I). After 2 days, the cells were fixed and immunostained with an anti-GLYT2 (A-F) or anti-GLYT1 antibody (**G-I**) that were visualized with an Alexa594-labeled secondary antibody (red). Images were acquired using a confocal microscope in the green and red channels, as indicated in the figure. A yellow color in the merged images signifies co-localization of the transporter constructs with the plasma membrane marker YFP-EAAT2. (**J**) Schematic representation of the transporter constructs used in which the numbers represent the initial and final residue included in the construct, according to the numeration of the corresponding wild type protein from which the different segments were derived. (**K**) COS cells were transfected with expression vectors for the constructs indicated in J. After two days, glycine uptake was determined by incubating the cells with 10 μM [^{3}H]glycine for 10 min at 37ºC. Values represent means ± S.E. of at least three triplicate determinations and are expressed as percentages of transport measured in cells transfected with GLYT2 wild-type.

Figure 2. Transport of glycine in mutants of the carboxyl terminus of GLYT1
(**A**) Multiple alignments using the ClustalW algorithm of the amino acid sequence of the carboxyl terminus of different NSS family members. The abbreviations are GLYT1-2, glycine transporter 1 or 2; PROT, proline transporter; BTGT, betaine transporter; GAT1-3, GABA transporters 1-3; NET, norepinephrine transporter; DAT, dopamine transporter; SERT, serotonin transporter. Identical or conserved residues are indicated with the symbols * or **:**, respectively. Residues that were mutated in the present study are indicated by arrows. (**B-C**) COS cells were transfected with expression vectors for the indicated wild-type or mutated forms of GLYT1 (B), or GAT1 (C), or GLYT2 (C). After two days, glycine or GABA uptake was determined by incubating the cells with 10 μM [^{3}H]glycine or 10 μM [^{3}H]GABA for 10 min at 37ºC. Values represent means ± S.E. of at least three triplicate determinations and are expressed as percentages of transport measured in cells transfected with the wild-type transporter.

Figure 3. Localization of wild-type and mutant GLYT1 expressed in MDCK cells

MDCK cells were transfected with wild-type GLYT1 or the carboxyl terminal GLYT1 mutants indicated. After two days, the cells were fixed and immunostained with the anti-GLYT1 antibody, which was visualized with an Alexa 488 labeled secondary antibody. Cells were observed using a fluorescence microscope and the images were collected with a CCD camera. Note the plasma membrane labeling of GLYT1wt, R575K, L576I, G569A and P582A (arrows) but the intracellular retention of mutants R575A, R575D and L576A. Mutant D585A is mainly intracellular but a weak plasma membrane staining is appreciated occasionally (arrow in **I**).

Figure 4. Delivery to the cell surface and transport activity of wild-type and mutant forms of GLYT1

(**A**) Cell surface biotinylation of wild-type and mutant GLYT1 expressed in MDCK cells. MDCK cells were transfected with wild-type GLYT1 (GLYT1wt), or R575A, or R575D, or L576A, or L576I or D585A mutants of GLYT1. After 2 days, cell surface proteins were labelled with the impermeable sulfo-NHS-biotin reagent and the biotinylated proteins were then recovered from lysates with streptavidin-agarose beads (see "Experimental"). The protein lysates (upper panel) or the biotinylated fractions (lower panel) were subjected to SDS-PAGE, electroblotted onto nitrocellulose, and incubated with anti-GLYT1 antibody. The protein bands were visualized using the ECL detection method and they corresponded to cell surface mature forms of GLYT1 or to the intracellular immature transporter, as indicated in the figure. (**B**) Comparison of transporter activity of GLYT1wt or the R575A, R575D, or L576A mutants in transfected COS cells or in reconstituted proteoliposomes. COS cells were transfected with the constructs indicated and two days later, glycine uptake was determined as in Figure1 (empty bars). Alternatively, the cells were solubilized, the protein reconstituted in proteoliposomes and glycine uptake was measured in these proteoliposomes (filled bars). The values represent means ± S.E. of at least three triplicate determinations and they are expressed as the percentage of transport measured in cells transfected with GLYT1 wild-type or in the proteoliposomes derived from these cells.

Figure 5. Localization of GLYT1 mutants and chimeras in MDCK cells

(**A-F**) MDCK cells were transfected with GFP-GLYT1R575A (G-R575A, green) (**A-C**) or with GFP-GLYT1wt (G-GLYT1wt, green) (**D-F**) and labeled with an anti-calnexin antibody as a marker of the endoplasmic reticulum (red). Colocalization was visualized as a yellow color in the merged images. (**G-I**) MDCK cells were cotransfected with YFP-EAAT2 (YFP-EAAT2, green channel) plus a GLYT2-GLYT1 chimera (G2-G1ct). The chimera was visualized with anti-GLYT2 antibody (red channel). (**J-L**) MDCK cells were cotransfected with YFP-EAAT2 (YFP-EAAT2, green channel) and a GLYT2-GLYT1R575A chimera (G2-G1R575A), and the chimera was visualized with anti-GLYT2 antibody (red channel). Note that the mutated chimera is retained in the intracellular compartment.

Figure 6. Interaction of GLYT1ct with Sec24D

(**A**) COS cells were transfected with *myc*-Sec24D and the cell lysate was incubated with either GST (GST), or GST-GLYT1ct (GST-G1ct), or GST-GLYT1ctR575A (GST-G1ctR575A), or GST-GLYT1ctD585A (GST-G1ctD585A), or GST-GLYT1ctL576A (GST-G1ctL576A) immobilized on glutathione-sepharose beads. Material bound to the beads was eluted with glutathione and analyzed by immunoblotting with anti-*myc* antibodies. The amount of GST fusion protein in the assays was monitored by Coomassie staining of the gel (lower panel). (**B**) The intensity of the bands obtained in the pull-down assay was quantified by densitometric analysis of the immunoblots. Values are presented as fold increase in the intensity of the bands over the value measured for the basal binding obtained with the control GST beads. Value are the means ± S.E. of three experiments.

Figure 7. Coexpression of wild-type and mutated GLYT1

MDCK cells were cotransfected with an HA-tagged form of the wild-type GLYT1 and either the GFP-tagged form of wild-type GLYT1 (G-GLYT1wt) (**A-C**), or GFPGLYT1 carrying the R575A mutation (G-R575A) (**D-F**), or GFPGLYT1 carrying the L576A mutation (G-L576A) (**J-L**). Controls were performed by cotransfecting the GFP tagged R575A (**G-I**) or L576A (**M-O)** mutants with HA-EAAT2. Two days later, the HA tag was immunolabeled in the cells which was visualized with an Alexa 594 labeled secondary antibody. GFP fluorescence is seen in green and HA immunofluorescence in red. Note that the transporter reached the plasma membrane in cells co-expressing GFP-R575A and HA-GLYT1wt (arrows in **D-F**) but not when it was coexpressed with HA-

EAAT2 (**G-I**). Similarly, the transporter reached the plasma membrane in cells co-expressing GFP-L576A and HA-GLYT1wt (arrows in **J-L**) but not when it was coexpressed with HA-EAAT2 (**M-O**)

Figure 8. Sucrose gradient analysis of GLYT1 oligomerization in rat brain synaptosomes. (A,B) 1 mg of rat brain synaptosomes were incubated in the presence of the membrane permeable cross-linker reagent DSS (5mM) (A), or the membrane impermeable cross-linker BS^3 (5 mM) (B). Synaptosomes were solubilized by incubation in RIPA buffer for 30 min and the unsolubilized material was removed by centrifugation at 100,000 x *g* for 30 min. The resulting soluble fraction was layered onto a 1-15% sucrose gradient (with a 25% sucrose cushion) and the gradient was centrifuged for 16 h at 150,000 x *g*. Fractions (0.5 ml) were collected from the bottom and the proteins were concentrated by precipitation with tricloroacetic acid. Proteins were resuspended in 100 µl of SDS-PAGE loading buffer. 30 µl of these samples were subjected to SDS-PAGE and immunoblotted with anti-GLYT1 antibody. The protein bands were visualized using the ECL detection method. Fractions are numbered from the top of the sucrose gradient. Arrowheads indicate the mobility of MW markers while m, d and t represent the expected mobility of GLYT1 monomers, dimers and tetramers, respectively. **(C)** Densitometric quantification of bands corresponding to monomers (●, ○), dimers (■, □) and tetramers (▲, Δ) in the presence of DSS (closed symbols) or BS^3 (open symbols). Values are referred to the maximum value measured for the monomer. Note that dimers and tetramers are about one order of magnitude less abundant than monomers. Values from fraction 5 are not included in the graph since the presence of abundant smeared protein precluded a precise quantification of the bands. This smear is probably due to the presence in this fraction of lipids reluctant to solubilization, since it was much higher in the absence of SDS in the solubilization buffer (not shown).

Figure 9. FRET microscopy in transfected cells

(**A-C**) COS cells were cotransfected with expression vectors for GLYT1YPetm and GLYT1CyPetm and, two days later, fluorescence emission from donor and acceptor were collected from living cells. FRET efficiency was calculated as indicated in "Experimental" and expressed as percentage and illustrated as pseudo-colored images.

Note that FRET efficiency is higher at the cell periphery. In some cells (**C**) higher efficiency was observed at intracellular compartments. (**D**) Histogram representing the mean values obtained for FRET efficiency in cells transfected with a tandem CFP-YFP (CY) (positive control), or CyPetm+YPetm (C+Y) (negative control 1), or EAAT2CyPetm+GLYT1YPetm (ET2C+G1Y) (negative control 2), or GLYT1CyPetm+GLYT1YPetm (G1C+G1Y). The FRET efficiency values were calculated over the whole area delimited by the cell contour. (mean ± S.E., *P < 0.001, paired t-test with negative control 1, n = 60).

Fernandez et al Figure 1

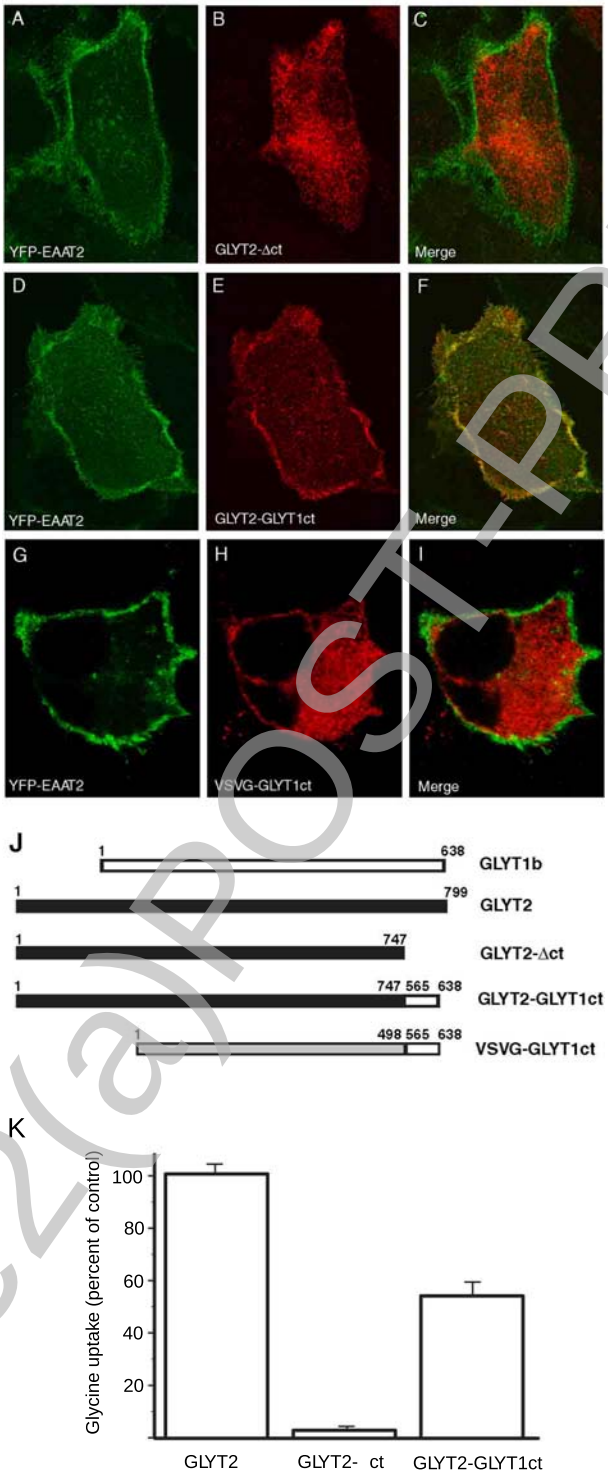

Fernandez at al Figure 2

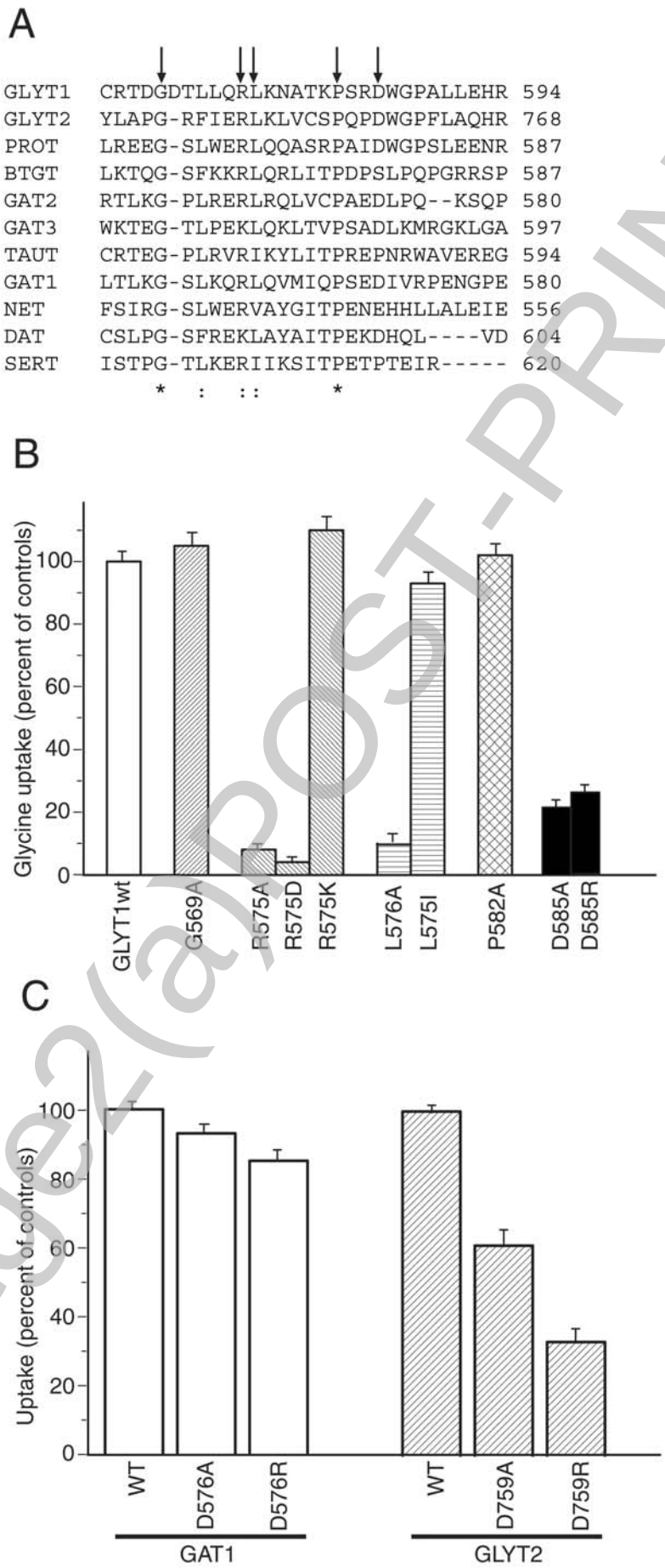

Figure 3

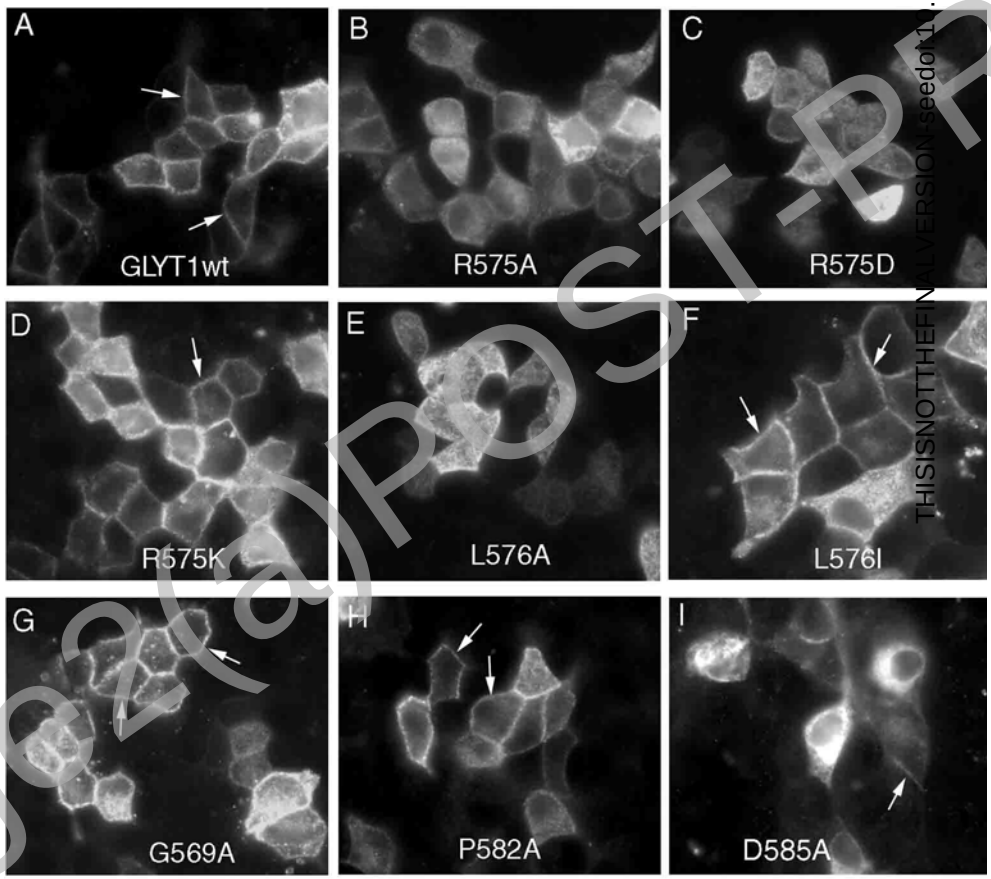

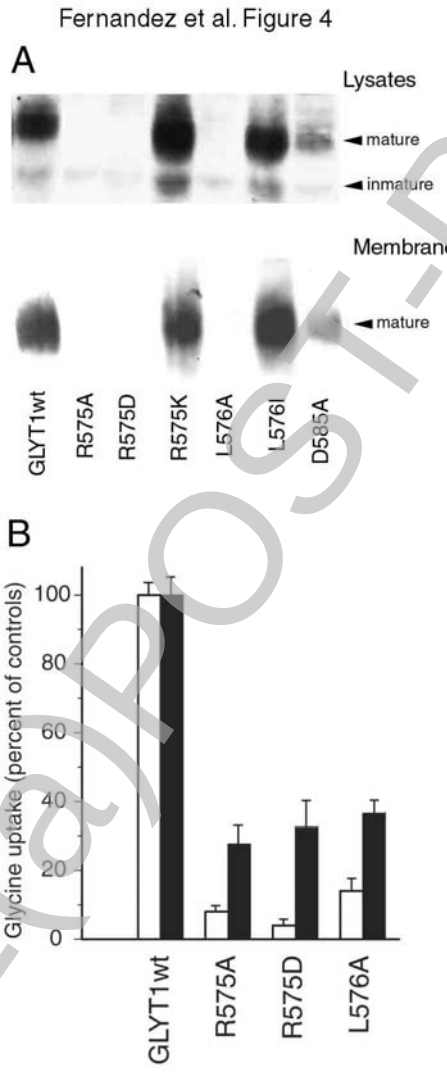

Fernandez et al Figure 5

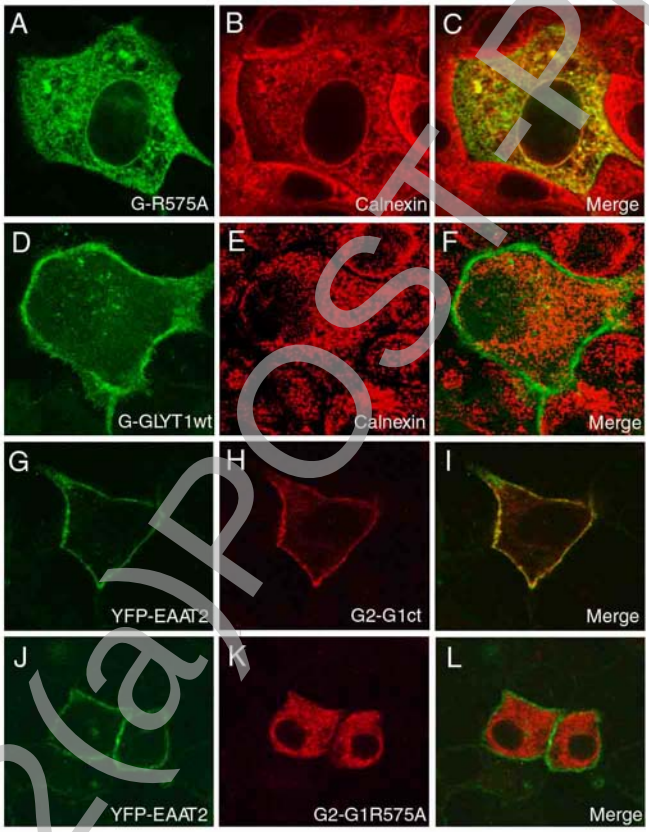

Fernandez et al Figure 6

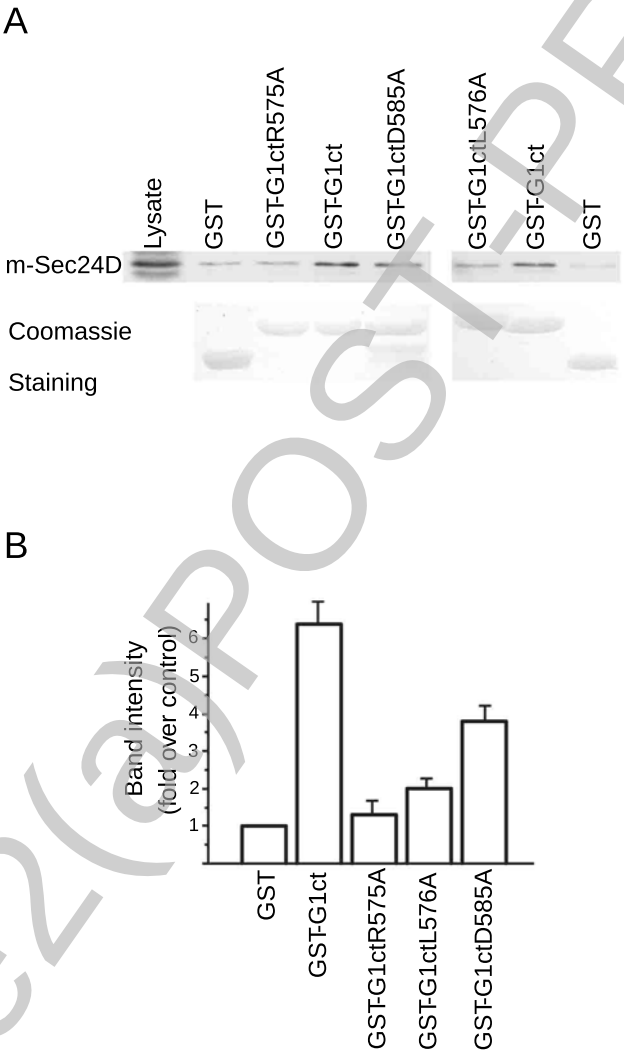

Fernández et al Fig. 7

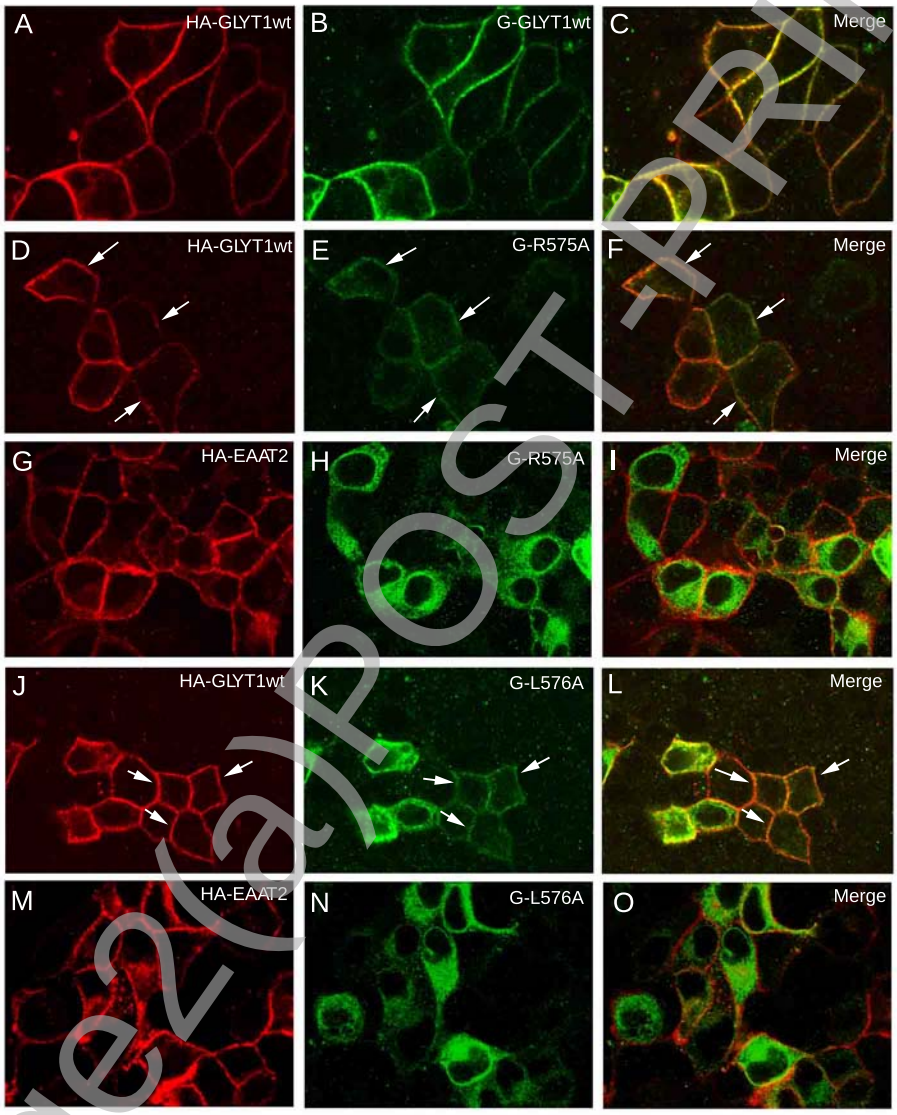

Fernández-Sánchez et al., Fig. 8

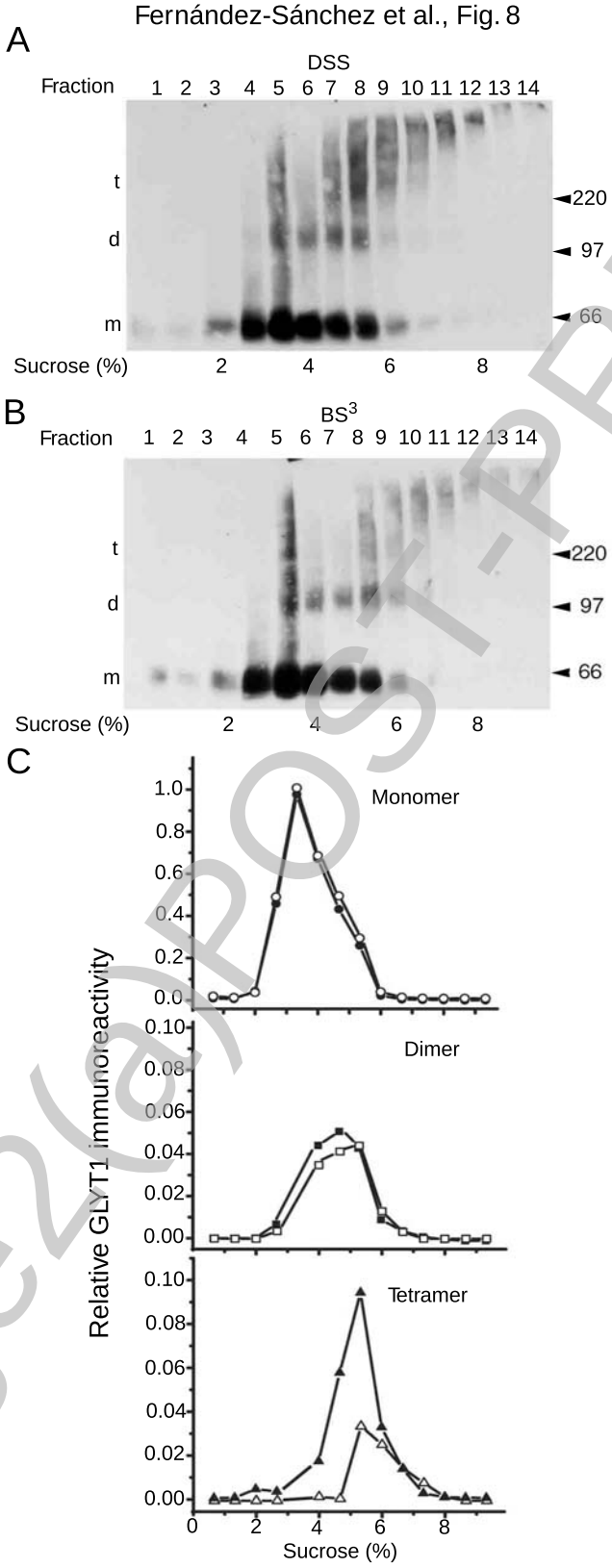

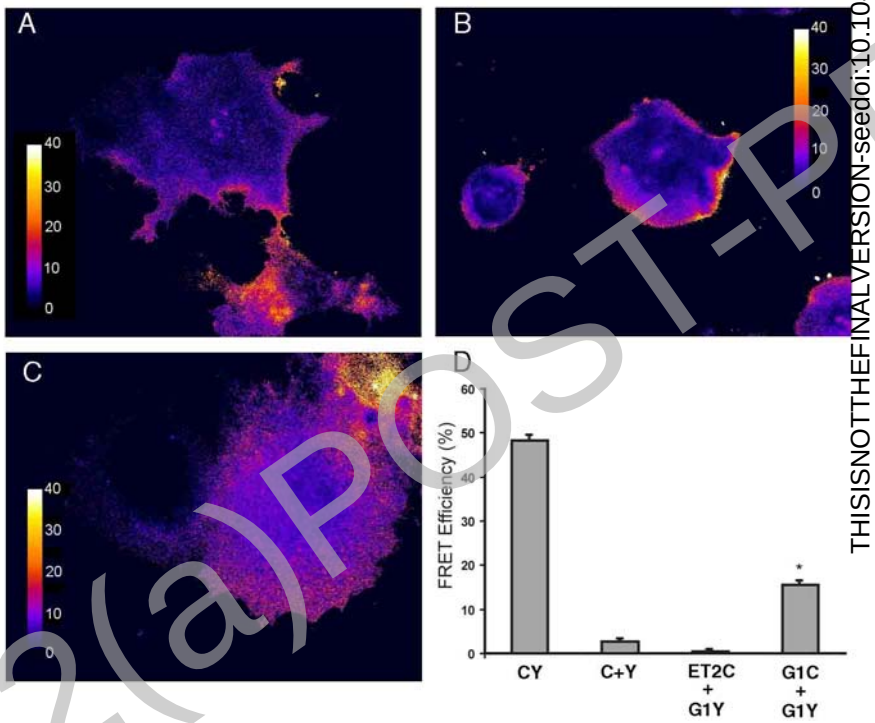

Fernandez et al Figure 9